Metaettringite, a decomposition product of ettringite

Q. Zhou, E.E. Lachowski, F.P. Glasser*

Meston Building, University of Aberdeen, Old Aberdeen, AB24 3UE, Scotland, UK

Abstract

Dehydroxylation of ettringite in an atmosphere of constant partial water vapour pressure (30–400 Torr) and controlled temperature (55–95 °C) yields an X-ray amorphous product containing 11–13 H_2O per ettringite formula unit. The X-ray amorphous product does, however, give electron diffraction patterns similar to those of ettringite but with a considerably reduced from $\sim$ 1.123 nm (ettringite) to 0.85 nm in the partially dehydroxylated product, termed metaettringite. The structure of metaettringite is closely related to that of fleischerite, $Pb_3Ge[(OH)_6](SO_4)_2 \cdot 3H_2O$ and the isostructural despujolsite, $Ca_3Mn^{IV}(SO_4)_2(OH)_6 \cdot 3H_2O$. These minerals contain columnar units. The columnar structure is like that of ettringite but with closer packing of columns in the a direction, resembling metaettringite.

The mechanism of collapse of ettringite to metaettringite, involving loss of water and motion of columns, cannot be achieved without scissoring and possibly rotation of individual columns; this and other defect-producing mechanisms result in loss of crystallinity of the metaettringite product.

© 2004 Elsevier Ltd. All rights reserved.

Keywords: Ettringite; Metaettringite; AFt phase; Thermal decomposition; Calcium sulfoaluminate hydrates

1. Introduction

Ettringite has been known from its natural occurrences since 1874 [1]; it is also a normal hydration product of ordinary Portland cements and is often abundant amongst the hydration products of sulfate-rich cements and in altered Portland cement. The amount of ettringite in Portland cement, its genesis, stability, morphology and microstructure, have been the subject of much recent investigation (e.g., Ref. [2]. The occurrence of ettringite has also been linked to "sulfate attack" on ordinary Portland cement as well as to delayed expansion in warm-cured Portland cement products. A recent book [3] reviews knowledge on the role of sulfate in cement.

The mechanism of decomposition of ettringite has been the subject of numerous studies, some under vacuum and some under hydrothermal conditions, but many are characterised by having exposed ettringite to isothermal decomposition at uncontrolled partial water vapour pressures. Since both temperature and water vapour pressure are key variables of the decomposition process, direct comparisons between different studies has not been possible. Decomposition releases water and, depending on sample size, packing and geometry, the release of water can result in locally elevated partial water vapour pressure, or in the appearance of transient liquid water, or both. The presence of liquid complicates the decomposition mechanism, inasmuch as dissolution–precipitation reactions leading to formation of AFm and a calcium sulfate phase, either gypsum or hemihydrate, are also known to occur [4].

The stable decomposition temperature of ettringite is in the range 114–116 °C [4,5]. At this point, liquid water is present at a pressure in excess of 760 Torr. In the presence of liquid water, as noted above, decomposition apparently occurs by a solution–precipitation mechanism, resulting in formation of sulfate AFm and hemihydrate, $CaSO_4 \cdot 0.5H_2O$. This pressure and temperature characterise an invariant point. The number of phases observed is five: ettringite, AFm, hemihydrate, aqueous and vapour. Applying the phase rule, $P + F = C + 2$, $C = 3$ (C_3A, $CaSO_4$ and H_2O) and therefore $F = 0$. Reaction kinetics are such that the equilibrium at the invariant point amongst solids ($C_3A \cdot 3CaSO_4 \cdot 32H_2O \rightleftharpoons C_3A \cdot CaSO_4 \cdot 12H_2O + CaSO_4 \cdot 0.5H_2O + 19.5H_2O$) is reversible although slow: decreasing the temperature slightly results in reconstitution of ettringite, also by a dissolution and reprecipitation process.

---

* Corresponding author.
E-mail address: f.p.glasser@abdn.ac.uk (F.P. Glasser).

However, in most practical applications ettringite decomposition is likely to be encountered at much lower temperatures than 114–116 °C because (i) total pressure only occasionally exceeds 760 Torr in cement service environments, (ii) the partial water vapour pressures of cements in their service environments, while variable, are normally less than saturation on account of dissolution in pore fluid of cement components, which reduce the activity of water. Concrete service temperatures exceed 50 °C only in exceptional circumstances. Exceptions to this temperature limit include cases where severe solar insolation occurs, perhaps enabling near-surface temperatures of 60–70 °C, and in deep, hot mines, where temperatures may reach 55–60 °C. These exceptions are clearly important to users, so there is interest in the kinetics and mechanisms of ettringite decomposition across a range of temperatures and partial water vapour pressures, but especially at water vapour pressures less than saturation such that water is essentially present either as vapour, or as crystal "water," or both.

Relevant studies in the literature can therefore be broadly divided into two classes: those made by treating ettringite in vacuum, in which P_{H_2O} is near zero, and those done either in self-generated atmospheres or with imposed pressure, under hydrothermal conditions. Datasets obtained in self-generated atmospheres are characterised by having been obtained at constant temperature, but at uncontrolled P_{H_2O} and it is therefore impossible to generalise on the stability of ettringite from their findings.

It is generally agreed that the first stage of water loss from ettringite is the loss of two of its maximum $32H_2O$: water contents are specified per six calciums. These two waters are zeolitic in the sense that they can be lost or gained reversibly without significant change in unit cell size or crystallinity. Changes in this range must therefore be determined by thermogravimetry and are not generally considered to represent decomposition, which only commences as water contents per formula unit decrease to less than $30H_2O$. This first stage of decomposition, the loss of zeolitic water, is encountered in both types of study.

In relevant previous studies describing the heating of natural ettringite [6], it was noted that "dehydration is accompanied by lattice shrinkage, mainly in the *ab* plane, giving a product with $a \simeq 0.84$ nm, $c \simeq 1.02$ nm and probable constitution $[Ca_3Al(OH)_6 \cdot 3H_2O]_2(SO_4)_3$" [7]. The same lattice shrinkage has apparently been observed in the vacuum of an electron microscope [7–9].

Skoblinskaya and Krasilnikov [8,9] describe the decomposition of ettringite in vacuum and identified four discrete stages. Initially, in the first stage, zeolitic water was lost, the water content decreasing from $31–32$ H_2O to $\sim 30H_2O$ per formula unit. In Stages 2 and 3, water bonded to calcium was lost in two stages, decreasing from $30H_2O$ to

$18H_2O$ and subsequently to $6H_2O$. The ettringite-like structure was said to be retained to water contents as low as $18H_2O$, but thereafter collapsed in the course of water loss between 18 and $6H_2O$. While external crystal morphology was preserved throughout decomposition, crystals were observed microscopically to crack and become amorphous between 18 and 6 H_2O. As the water content decreased to $\sim 18H_2O$, *a* decreased markedly with smaller contraction of *c*, although progressive degradation of the structure and consequent reduction in the quality of the diffraction pattern prevented accurate measurement of the lattice parameters subsequent to the initial stages of water loss.

Zhou and Glasser [4] examined ettringite stability and the reversibility of ettringite decomposition at controlled P_{H_2O}. They found that decomposition and reformation occurred reversibly, but only with hysteresis, in the range 30–400 Torr and at temperatures between 55 and 95 °C [4]. Fig. 1 shows a typical isobaric diagram for ettringite decomposition and formation under these conditions: arrows show directions of temperature change. It is specially relevant to the present treatment to note (i) the large area of water contents/temperatures included within the region bounded by decomposition and reformation curves and (ii) the relative constancy of water content of the partially dehydrated product obtained over a range of temperatures: these same characteristics, including near constancy of water contents in the range 11–13 H_2O, occur on other isobars. In the course of the present study it was found that decomposition on selected isobars in the range of water vapour pressures 30–400 Torr gave an apparently homogeneous product amorphous to X-ray diffraction but crystalline to electron diffraction. This product is termed "metaettringite" and this paper presents additional data for its characterisation, its mode of formation and structural relationships to its precursor as well as other mineral phases.
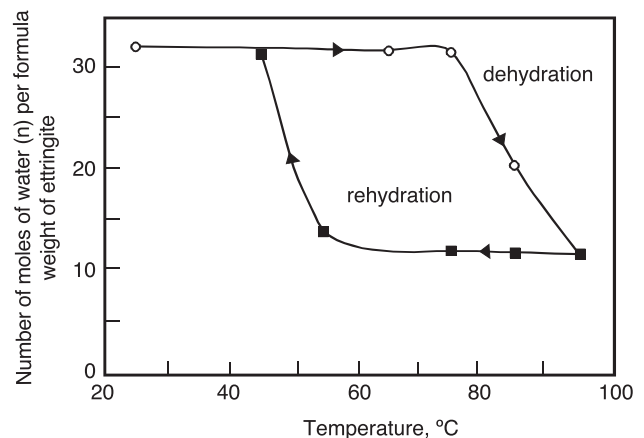

Fig. 1. An isobaric plot showing the water content of ettringite compositions at $P = 75$ Torr. Arrows show the direction of semistatic temperature change.

2. Results

2.1. Preparation of ettringite

Ettringite was prepared by reacting tricalcium aluminate, prepared in a previous operation by ceramic sintering at ~ 1350 °C of reagent grades of $CaCO_3$ and Al_2O_3, with reagent-grade $CaSO_4 \cdot 2H_2O$. The two solids were mixed into slurries with degassed, deionised water. In a typical preparation, 0.02 moles of C_3A were mixed with 0.06 moles of gypsum and slurried into 1 l of water. After 10 days of gentle agitation at 20 ± 2 °C in a closed vessel, so as to exclude CO_2, the precipitate was filtered, dried in CO_2-free air and checked for purity by X-ray diffraction. Optical and electron microscopy disclosed that the product consisted almost entirely of needles and prisms up to $10-20$ μm in length. Only traces of amorphous material persisted, as evidenced by crystallite morphology and selected area electron diffraction.

2.2. Conversion of ettringite to metaettringite

A free-flowing ettringite powder, ca. $100-1000$ mg, was placed in a regulated system in which both temperature and water vapour pressure ($P_{H_2}O$) were controlled. Flowing gas at constant $P_{H_2}O$ was continuously introduced to either sweep away water vapour arising from ettringite decomposition or supply water for its reconstitution while maintaining essentially constant humidity near the solid sample. Typically, after 6 days dehydration of ettringite at 95 °C and $P_{H_2}O = 75$ Torr, the product had a water content $n = 11.6$ and appeared to be completely amorphous to powder X-ray diffraction.

At $P_{H_2}O = 75$ Torr, and upon decreasing the temperature to 45 °C while maintaining constant $P_{H_2}O$, metaettringite regenerated to ettringite with $n = 30.8$ within 12 days. This general behaviour, of reversibility only with significant hysteresis, was observed on other isobars in the range $75-400$ Torr.

2.3. Selected area electron diffraction

Specimens were prepared by dispersing ettringite in 2-propanol with ultrasonic agitation and then drying a drop of the resulting suspension on a copper mesh grid that had a carbon, or carbon–aluminium support film. The Al served as an internal d-spacing standard. The specimens were examined in a JEOL 2000 EX Temscam microscope, operated at 2000 kV. Ettringite that had been dehydrated until only $11-13$ water molecules remained per formula unit was amorphous to X-rays, although electron diffraction
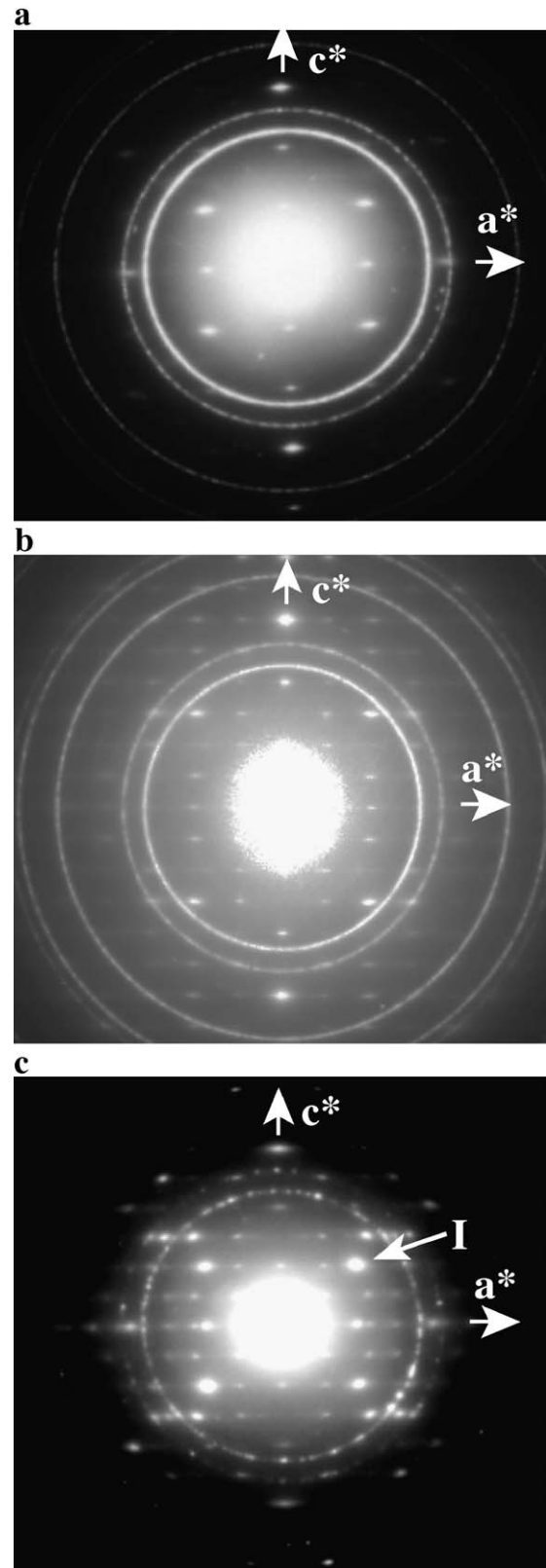

Fig. 2. (a) SAED pattern showing only a few strong diffraction spots. These correspond to a cell having $a = 0.94$ nm and $c = 0.06$ nm by analogy with ettringite, although there is no evidence for centering in the pattern. (b) SAED pattern of metaettringite showing an array of weak diffraction spots. Spacings indicate $a = 0.83$ nm and $c = 0.98$ nm. (c) SAED pattern showing a from a single crystal of metaettringite. The strong spots (1) are incommensurate with the array of weaker spots and the pattern is composed of a mixture of the features in (a) and (b).

patterns could be obtained from well-morphed former crystals, the external morphology of which was preserved. There was some variability in the patterns obtained, some laths and needles having more reflections than others, as well as point-to-point variation within individual crystals, but all diffraction patterns had many features in common. These variations could be explained by a superposition of the two diffraction patterns shown in Fig. 2. Fig. 3 is a dark-field image of a former crystal and it reveals that only that part of the lath (bright in the micrograph) contributes to the diffractions.

Dehydroxylation of ettringite to less than 30 H_2O can occur at relatively high partial water vapour pressures, 75 Torr in this study. Nevertheless, with great care, metaettringite can be handled in the high vacuum of the electron microscope without significant decomposition provided that the exposure time is brief and beam intensities are kept low to minimise heating. The crystals do, however, become amorphous on prolonged exposure to the beam and it was not possible to do tilting experiments to determine the true unit cell or cells, so the axes are defined by analogy with normal ettringite as defined in Ref. [10]. Beam damage effects are, to the best of our ability, excluded from the results.

Measurements of c in several crystals whose water content had been reduced to $11-13$ H_2O produced a range of values from 1.054 to 1.069 nm, very close to half the value for normal ettringite (2.1408 nm). This halving of c may readily be explained by disorder amongst the intercolumnar sulfate and by loss of zeolitic water. There is little sign of disorder along c^* in the diffraction patterns and also (00l) reflections where l is odd are weak or missing. This strongly suggests that the $Ca_3Al(OH)_6^{3+}$
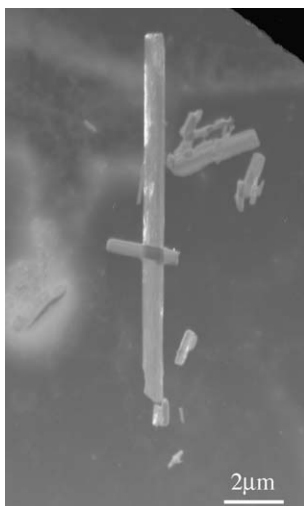

Fig. 3. Dark-field electron micrograph of ettringite previously dried to 11H_2O molecules per unit cell. The image was made using (004) diffraction spot from the long, vertical lath. Areas contributing to the diffraction spot are bright. Dark areas may be amorphous or not suitably oriented for diffraction.

cationic columns remain essentially intact at this stage of the dehydroxation.

The situation in the a direction is rather more complicated. There is considerable streaking indicative of disorder parallel to a^* (see Fig. 2c); measurements indicate the presence of two interpenetrating lattices with incommensurate reflections. For example, the diffraction pattern shown in Fig. 2c contains a mixture of the features found in both Fig. 2a and b, but occurring within an individual single crystal. Deconvolution of the two patterns suggests the following interpretation: one lattice has fairly even intensities and a repeat of about 0.735 nm (a^*), which corresponds to $a = 0.849$ nm, in good agreement with previous findings [8,9]. This is roughly the distance that would be obtained if the $[Ca_3Al(OH)_6]^{3+}$ columns were touching. The patterns also had a second array of diffractions (some are labelled in Fig. 2c), incommensurate with the first along a^*, but commensurate along c*. The intensities are very uneven, to such an extent that rows with $h = 1$ are not discernible; the repeat along a^* is thus 0.852 nm, making $a = 0.984$ nm. However, it is difficult to explain the lack of reflections along c^* in Fig. 2a. One possibility is that c is further reduced by slight displacement of the Ca atoms at 1 and 2 such that they become crystallographically equivalent (see Fig. 5a). However, this explanation is rendered implausible by the fact that, at further dehydration levels, the repeat along c is once more two cage units. The alternative explanation, of systematic absences caused by enhanced symmetry, is equally implausible.

The above suggests that the columns are essentially preserved with very little displacement along c, but displacement and shrinkage occurs mainly along a as water is lost from the intercolumnar region. This displacement appears to occur stepwise to account for the two interpenetrating lattices.

In order to solve the crystal structure of metaettringite, we first attempted to construct a computer-based model using the program ATOMS [11], which maintained the column architecture while enabling a computer-generated protocol to be applied that shifted columns closer together, with elimination of water, while at the same time preserving electroneutrality. This solution converged on two models, one of which was essentially identical in all respects, allowing for differences in size of the relevant atoms or groups, with the known structures of despujolsite, $Ca_3Mn^{4+}(SO_4)_2(OH)_6 \cdot 3H_2O$, fleischerite, $Pb_3Ge^{4+}(SO_4)_2(OH)_6 \cdot 3H_2O$ and schaurterite, $Ca_3Ge^{4+}(SO_4)_2(OH)_6 \cdot 3H_2O$ (collectively termed dfs phases), all with symmetry P62c [12]. The dfs structure, like that of metaettringite, contains 12H_2O per six calcium atoms and is constructed of columns geometrically identical in principle with those of ettringite, although more closely spaced in the a direction. Given the apparent stability of this structure for a wide range of chemistries, although not those typical of ettringite-like phases, as well as the convergence of computer-generated models in this arrangement, it becomes our preferred model for the structure of metaettringite. However,

Table 1
Specific BET surface area (m^2/g) of ettringite and metaettringite

Outgas procedure and water content		After 24 h, 95 °C, P_{H_2O} = 75 Torr
19 h, 20 °C in poor vacuum	4.50 (30H$_2$O)	5.04 (13H$_2$O)
168 h, 20 °C over anhydrous CaC$_2$	4.58 (30H$_2$O)	4.94 (13H$_2$O)
3 h D-drying (vacuum at dry ice–acetone temperature)	4.46 (30H$_2$O)	4.83 (13H$_2$O)

the possibility of alternate structures remain; describing partially dehydrated ettringite the type locality, Ettringen, Germany, in Ref. [6], these authors note that the product they obtained by dehydration in the laboratory was "not identical with dehydrated ettringite."

Table 1 records the BET surface areas of fresh ettringite, containing 30H$_2$O, and of metaettringite prepared at 90 °C from this ettringite precursor. Small but significant increases in specific surface occur in the course of conversion of ettringite to metaettringite. The additional surface area is believed to reflect the defect nature of metaettringite, the difference representing additional sites created in the course of the decomposition that are favourable for N$_2$ sorption.

3. Discussion

The existence of a special class of transformations, termed "topotactic," have long been recognised. In this context, topotactic refers to a transformation that preserves crystal structure in three dimensions even though in the course of transformation, nominally structurally essential constituents are lost [13]. In this example, ettringite loses approximately 18 of its essential water molecules, the water content decreasing from 30H$_2$O (two additional water molecules may be present but are zeolitic) to about 12H$_2$O. In the course of transformation the columns, $[Ca_3A\ell(OH)_6]^{3+}$, are preserved but as intercolumnar water is lost, individual columns move closer together; charge-compensating sulfate is preserved but may be mobile. In this instance, the preferred new arrangement proves to be stable for some compositions, e.g., minerals of the dfs family but not presumably for ettringite. Nevertheless atomic migration is minimised by formation of a metastable phase and decomposition proceeds:

$$\text{ettringite} \rightarrow \text{dfs} - \text{structured phase} + 18H_2O$$

Figs. 4 and 5 contrast the structures of ettringite and of a dfs phase, in this instance, despujolsite, in plan and projection relative to *c*. The 12H$_2$O model, that of a dfs phase, is essentially identical with initial attempts to create a structure by computer synthesis with controlled movements of the columns.

The mechanism of transformation may be envisaged as follows: If, in addition to the intercolumnar water, all the apical water molecules at 3 and half of those at 4 are removed (Figs. 4a and 5a), the columns may approach and fuse by hydrogen bonding of the remaining apical water molecules. Only water molecules are removed, so that the charge balance is not affected. The residual water content corresponds ideally to an empirical formula of $C_3A \cdot 3CaSO_4 \cdot 12H_2O$. The diameter of a fully hydrated column, from apical oxygen to oxygen, is 0.67 nm, so the closest possible approach of columns would correspond to a value for *a* of 0.77 nm. The observed value, 0.849 nm, is somewhat larger than this because of the need also to accommodate other ions, including charge-balancing sulfate ions, in the intercolumnar spaces.

The resulting structure of metaettringite is thus believed closely to resemble that of a dfs phase, for example, despujolsite, $Ca_6Mn_2^{IV}(SO_4)_4(OH)_{12} \cdot 6H_2O$ (Figs. 4b and 5b), which is hexagonal with *a* = 0.856 nm and *c* = 1.076 nm. The unit cell is thus comparable to that suggested for metaettringite: while the structure of despujolsite contains columns similar to those in ettringite, it has Mn^{IV} in place of Al. These columns are not isolated, but are joined by apical water molecules corresponding to those marked 4 in the ettringite structure (Figs. 4a and 5a) and also by sulfate ions, whose O atoms are bonded to the calcium ions in positions corresponding to the ettringite apical water molecules at position 4: not all of the apical water molecules are present in despujolsite. The columns are also rotated with respect to those in ettringite. It is not necessary that water molecules are lost from particular sites in the transformation of ettringite to metaettringite as rearrangement of the intracolumnar species may occur in the course of transformation.

However, there is another possibility to achieve the packing of columns in metaettringite, achieved by removal of all the apical water molecules at 3 and half of those at 4 (Figs. 4a and 5a). The columns may then share water molecules without rotation. The diffraction data cannot distinguish between the two possibilities and we cannot determine the position of the sulfate that, in any event, may be disordered as occurs in fleischerite. Observations in the literature point to the possible existence of several types of metaettringite but we have been unable to source naturally occurring metaettringite, the existence of which was reported in Ref. [6].

At lesser water losses, the presence of more of the apical water molecules prevents the full approach of the columns and accounts for the progressive reduced shrinkage of the unit cell along *a*. The incommensurate diffraction spots suggest that a common occurrence amongst crystals undergoing decomposition is the development of coherent domains at intermediate stages of decomposition, the domains differing in water contents. Thus, in bulk, the transformation may appear to proceed with continuous loss of water but transformation actually
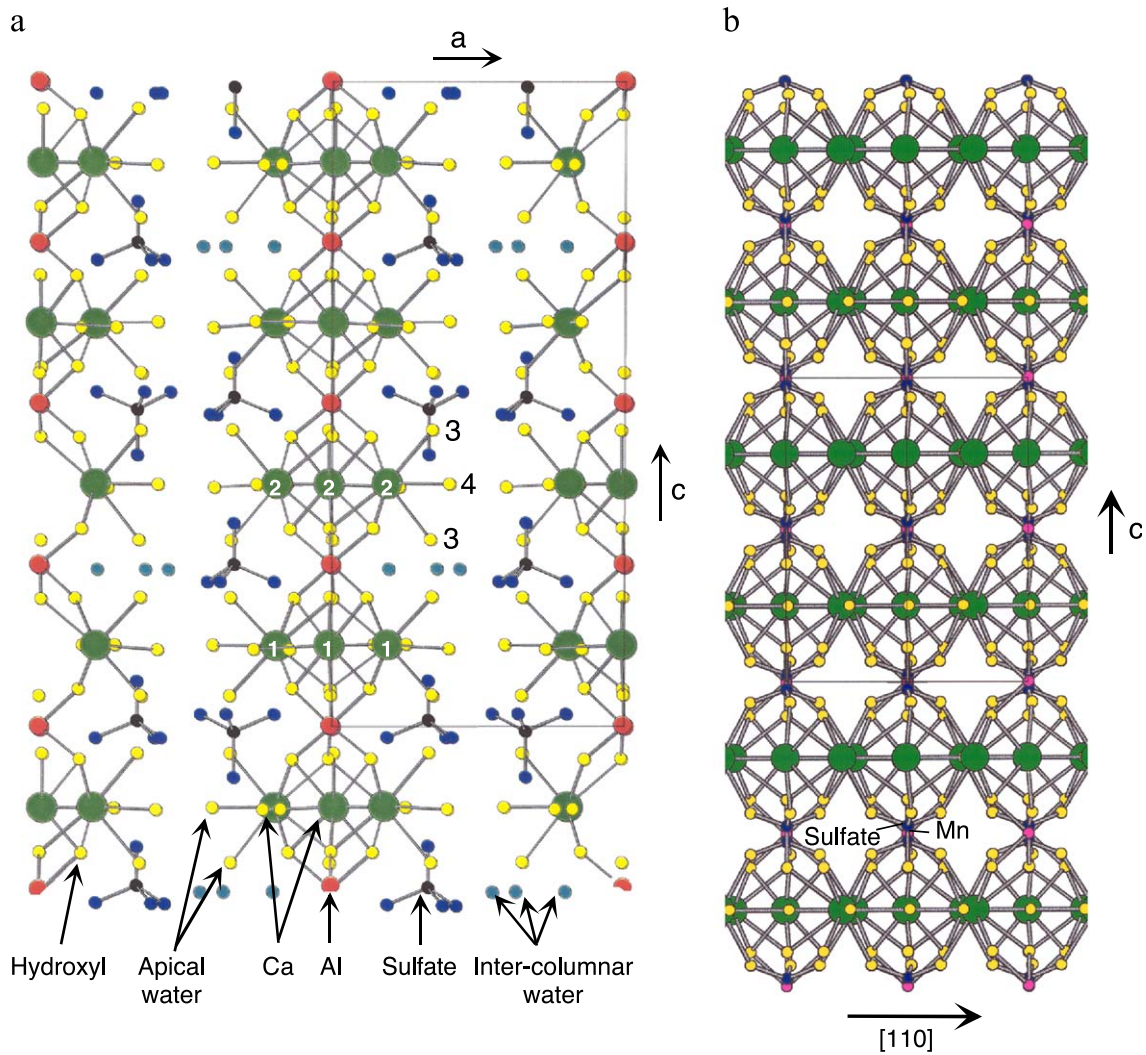
Fig. 4. (a) Crystal structure of ettringite, viewed along *a*; unit cell is outlined. Structure data from Moore and Taylor [10]. (b) Crystal structure of despujolsite, rotated round *c* to show cages. From Gaudefroy et al. [12].

proceeds on a microscale or nanoscale by formation of discreet domains.

Thus, gradual collapse of columnar material in ettringite undergoing decomposition is unlikely to be a continuous process occurring homogeneously throughout the bulk of the crystal. Water loss initiates primarily at the surface or near the surface of crystal individuals: faces parallel to *c* are morphologically most prominent and probably allow water to escape at the outset. While the water in intercolumnar channels is probably mobile in the active stages of decomposition, composition gradients undoubtedly occur in the course of the transformation.

Sulfate ions appear to exhibit a range of ordering in phases of the dfs family; disordering of sulfates presumably occurs in ettringite in the course of its conversion to metaettringite and is believed to assist the structure in maintaining local electroneutrality, while at the same time it facilitates templating adjacent columns into their new locations.

However, the process comprises a sufficiently drastic rearrangement as not to be accomplished without significant structural degradation. Disorder along *a*, evidenced from electron diffraction, supports this contention. It is likely, therefore, that columns become broken during transformation with the result that the principal misalignments occur in the *a* direction. As a consequence, defects are introduced that are manifested in the increased BET surface areas. If, however, water loss had occurred with maintenance of column spacing, corresponding to little change in crystallographic *a*, a very large increase in space accessible to nitrogen should have occurred. That only a small increase is actually recorded is a measure of structural coherence is the final arrangement.

The hysteresis loop in the decomposition $P_{H_2O}-T$ plot (Fig. 1) results because the decomposition does not occur under equilibrium conditions. However, the present study defines more precisely the structural states of the solid(s) at intermediate stages of decompositon. The stages and mechanisms involved are illustrated in Fig. 6. The hysteresis loop
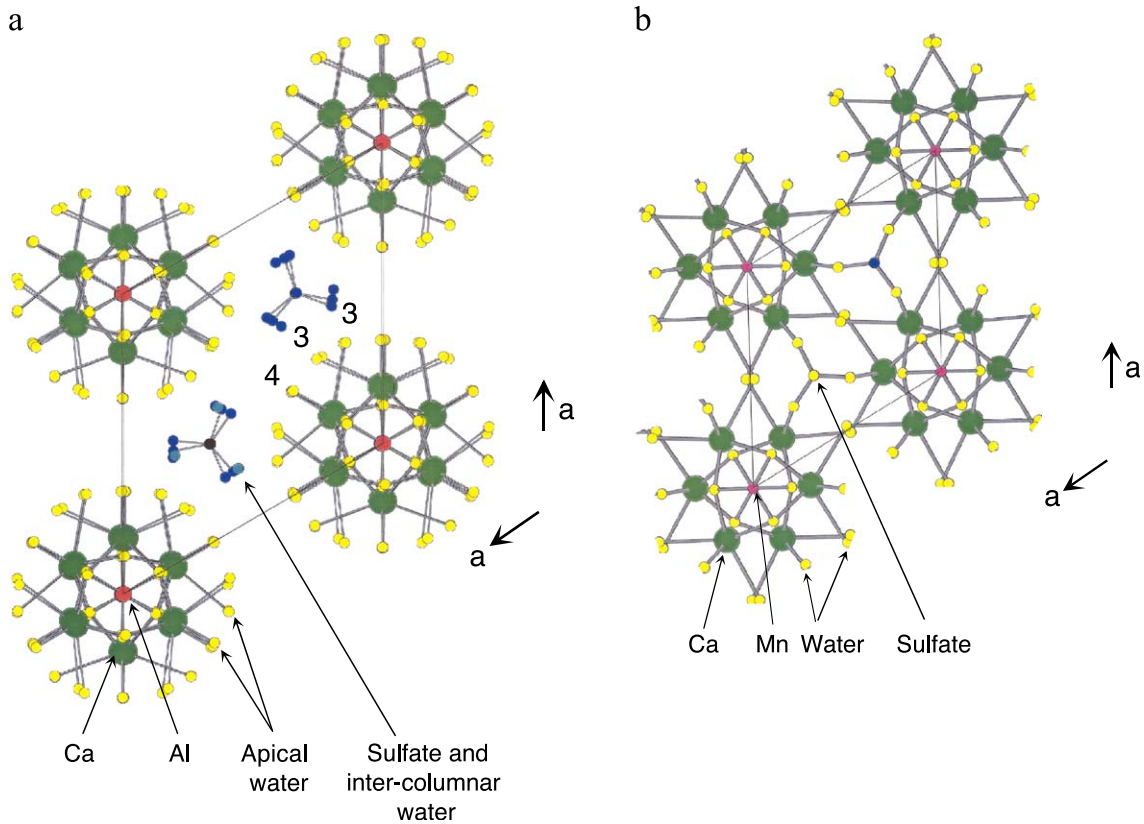
a

b

Fig. 5. (a) Crystal structure of ettringite viewed down *c*. (b) Crystal structure of despujolsite viewed down *c*. Note the rotation of the columns relative to those in Fig. 4a.

for formation and decomposition, an example of which is shown in Fig. 1, is generated as a result of different mechanisms for decomposition and reformation: on the heating cycle, previously formed ettringite decomposes topotactically to a metastable but persistent phase, metaettringite. Therefore, to reform ettringite at constant P_{H_2O} it is necessary to decrease the temperature. It is speculated that in practice, the decrease needs to be sufficient to permit capillary condensation to occur on crystal surfaces and at the site where mosaic boundaries of the nanoscale crystallites intersect the morphological surfaces. The preferred product of recrystallisation is ettringite, the stable phase under these conditions. It is thus not practicable to determine an actual equilibrium decomposition temperature on any isobar, although the equilibrium must lie somewhere between the two temperatures shown, the upper for decomposition and the lower for ettringite reformation. If, however, liquid water accumulates either in the initial states of decomposition or by condensation from vapour, dissolution/recrystallisation occurs as shown by a different pathway.

Metaettringite is isostructural with dfs minerals although considerably less well ordered. Synthesis of the dfs phases has been reported: coupled with their occurrence in nature, we suppose them to have a definite but as yet undefined
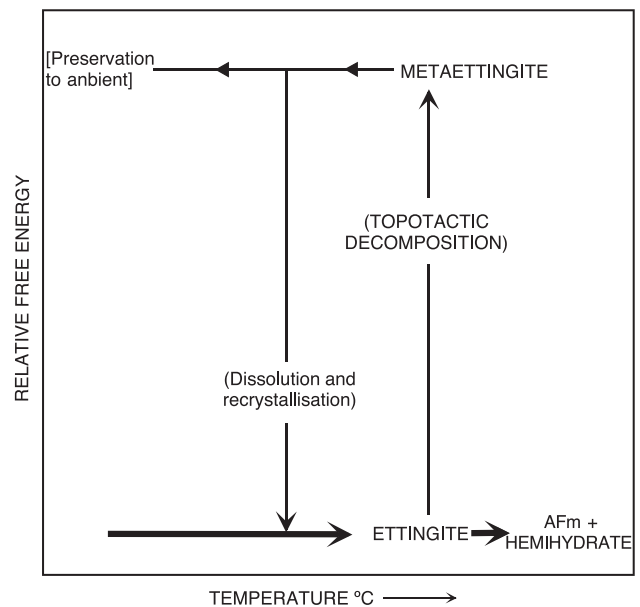

Fig. 6. Isobaric (P_{H_2O}) diagram of decomposition processes affecting ettringite. Stable pathways are shown in bold, near the bottom. Suggested mechanisms are described in the text. Mettaettringite has occasionally been observed upon prolonged treatment to nucleate AFm, but conditions for this to occur are not sufficiently well defined to place on the diagram.

stability range. However, metaettringite appears to be metastable under all conditions thus far studied. But its discovery and elucidation, coupled with identification of the stable dfs phases highlights the possibility of constructing networks having essentially identical columnar constructions, but with different columnar spacings and, of course, intercolumnar contents, especially with respect to the content of neutral molecules, e.g., water. Other factors being equal, the *a* spacing would, it is supposed, be related to differing water contents, larger spacings demanding higher water contents. The only two columnar spacings thus far known to exist— minerals of the ettringite and dfs families, including metaettringite—may not complete the picture and other phases containing essentially the same columns but differing in columnar spacings and with characteristically different water contents may remain to be discovered. These columnar phases are remarkably flexible and stable and the possibility exists that columnar arrangements with even higher water contents than ettringite remain to be discovered.

Acknowledgements

References

[1] R.V. Gaines, H.C.W. Skinner, E.F. Foord, B. Mason, A. Rosenzweig, Dana's New Mineralogy, 8th ed., John Wiley, New York, 1998.

[2] F.P. Glasser, The stability of ettringite, Proceedings of Rilem Meeting on Delayed Ettringite Formation, Villars-sur-Ollon, Switzerland, Sept. 4–6, 2002, in press.

[3] J. Skalny, J. Marchand, I. Odler (Eds.), Sulfate Attack on Concrete, Modern Concrete Technology Series, vol. 10, E. & F. Spon, London, 2002.

[4] Q. Zhou, F.P. Glasser, Thermal stability and decomposition mechanisms of ettringite at <120 °C, Cem. Concr. Res. 31 (2001) 1333–1339.

[5] C. Hall, P. Barnes, A.D. Billmore, A.C. Jupe, X. Turrillas, Thermal decomposition of ettringite, $Ca_6[A\ell(OH)_6]_2(SO_4)_3 \cdot 26H_2O$, J. Chem. Soc., Faraday Trans. 92 (12) (1996) 2125–2129.

[6] F.A. Bannister, M.H. Hey, J.D. Bernal, Ettringite from Scawthill, Co Antrim, Miner. Mag. 24 (1936) 324–329.

[7] J.A. Gard, in: H.F.W. Taylor (Ed.), Chemistry of Cements, vol. 2, Academic Press, London, 1962, pp. 243–270. Chapter 24.

[8] N.N. Skoblinskaya, K.G. Krasilnikov, Changes in crystal structure of ettringite on dehydration, 1, Cem. Concr. Res. 5 (4) (1975) 381–394.

[9] N.N. Skobinskaya, K.G. Krasilnikov, Changes in crystal structure of ettringite on dehydration, 2, Cem. Concr. Res. 5 (5) (1975) 419–432.

[10] A.E. Moore, H.F.W. Taylor, Crystal structure of ettringite, Acta Crystallogr., B 26 (1970) 386–393.

[11] Atoms Union 5.0.7 © Eric Dowtry, 1999.

[12] C. Gaudefroy, M.M. Granger, F. Permingeat, J. Protas, La despujolsite, une novelle espece minerale, Bull. Soc. Fr. Mineral. Cristallogr. 82 (1968) 43–50.

[13] L.S. Dent, F.P. Glasser, H.F.W. Taylor, Review on topotactic reactions in inorganic oxy-compounds, Q. Rev. 16 (43) (1962) 43–60.